Effect of strain on structure and charge order transitions in epitaxial $Bi_{0.4}Ca_{0.6}MnO_3$ films on perovskite (001) and (011) substrates

Dae Ho Kim,[a] Hans M. Christen, Maria Varela, Ho Nyung Lee, and Douglas H. Lowndes
Materials Science and Technology Division, Oak Ridge National Laboratory, Oak Ridge, Tennessee 37831

(Received 2 March 2006; accepted 22 April 2006; published online 18 May 2006)

The effect of epitaxial strain on the charge order (CO) transition in $Bi_{0.4}Ca_{0.6}MnO_3$ films was studied by varying the strain's strength and symmetry via the use of $SrTiO_3$ and $LaAlO_3$ substrates having different crystallographic orientations. The film on pseudocubic (001) $LaAlO_3$, under symmetric compressive strain, exhibits a clear CO transition. In the film on a (001) $SrTiO_3$ substrate, under symmetric tensile strain, highly segregated line-shaped features in the Bi distribution are seen in Z-contrast scanning transmission microscopy, accompanied by a strongly broadened CO transition. The asymmetric tensile stress on (011) $SrTiO_3$ results in an apparent compressive strain state with a deviation from tetragonality (i.e., $\gamma \neq 90^\circ$), accompanied by the sharpest CO transition. These comparisons illustrate the importance of considering both the strength and symmetry of epitaxial strain. © *2006 American Institute of Physics*. [DOI: 10.1063/1.2205753]

The relationship between epitaxial strain and phase transitions, such as charge order (CO) in manganite thin films, has been the subject of numerous investigations.[1,2] CO in manganites, wherein electrons become localized on specific lattice sites due to the ordering of Mn^{4+}/Mn^{3+}, is governed by Jahn-Teller distortions and orbital degrees of freedom, and thus is highly susceptible to structural distortions.[3,4] Consequently, epitaxial strain can be used to deliberately modify and potentially enhance such properties in complex oxides. Most research in this area has focused on using various substrates with different in-plane lattice parameters while preserving the in-plane square lattice, resulting in isotropic (biaxial) tensile or compressive strain.[1,2] However, substrate surfaces that are oriented in a lower-symmetry plane provide additional freedom and asymmetry. For the case of epitaxy on (011) GaAs, strain states fundamentally different from those obtained on symmetric planes were observed.[5] In perovskites, the use of (011) $SrTiO_3$ (STO) is further motivated by the fact that it lacks the potentially complicating aspect of charge imbalance at interfaces between dissimilar perovskites.[6] Recently, Wakabayashi *et al.* have reported a unique charge orbital ordering induced by anisotropic stress in a $Nd_{0.5}Sr_{0.5}MnO_3$ thin film grown on such a (011) STO substrate.[7] In a series of papers, they showed that the application of asymmetric strain, and the freedom to form crystalline structures with a nonsquare basal plane, provides structural flexibility that is indispensable for the large anisotropic lattice deformation that occurs at the first-order CO transition.[8,9]

$Bi_{1-x}Ca_xMnO_3$ has been studied extensively for its strong CO and intriguing ferromagnetism at $x=0$.[10,11] The triclinic crystal structure of $Bi_{1-x}Ca_xMnO_3$ can be represented as a slight deviation from a tetragonally distorted perovskite lattice, with $c/2<a=b$ for $x>0.45$ (and $c/2>a=b$ otherwise), and $90^\circ<\alpha=\beta<\gamma<91^\circ$.[12] $Bi_{0.4}Ca_{0.6}MnO_3$ (BCMO) is particularly interesting for its high CO transition temperature (~330 K) and photoinduced resistivity changes.[13] Bulk lattice parameters are $a=b=3.81$, $c=2\times3.79$ Å just above the CO transition (i.e., a unit cell volume of 54.94 Å^3), and $a=b=3.83$, $c=2\times3.77$ Å just below.[12] While the unit cell volume changes only insignificantly at the CO transition, the distortion $(c-2a)/c$ increases significantly. Therefore, it is interesting to investigate how the constraint of epitaxially induced strain will affect this transition.

Epitaxial BCMO films were grown onto (001)- and (011)-oriented STO and $LaAlO_3$ (LAO) substrates by pulsed laser deposition. Through out this letter, the pseudocubic notation is used for LAO substrates. A sintered polycrystalline $Bi_{0.4}Ca_{0.6}MnO_3$ target with 25 at. % excess Bi was ablated with a KrF excimer laser ($\lambda=248$ nm) while the substrate temperature was kept at 700 °C and the oxygen pressure at 200 mTorr. The thicknesses of the films range from 300 to 500 nm. Four-circle x-ray diffraction (XRD) and Z-contrast scanning transmission electron microscopy (Z-STEM) observations (performed in an aberration-corrected VG microscopes HB501UX dedicated STEM) show that the films are epitaxial on both kinds of the substrates.

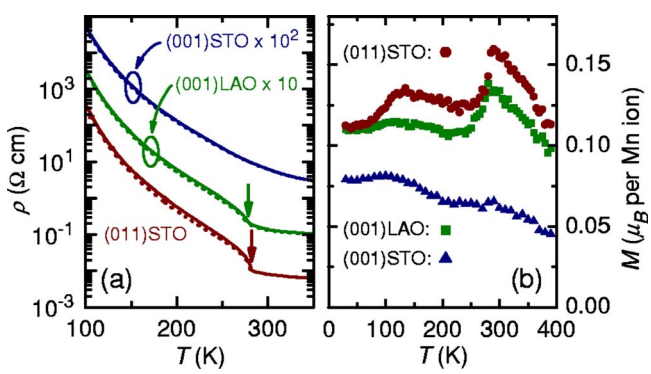

FIG. 1. (Color online) (a) Temperature dependence of the resistivity for the $Bi_{0.4}Ca_{0.6}MnO_3$ films on (001) $SrTiO_3$ (blue), (001) $LaAlO_3$ (green), and (011) $SrTiO_3$ (red) substrates. The solid (dashed) lines are measured upon heating (cooling). The arrows indicate charge order transitions. (b) Temperature dependence of the magnetization measured at 4 T for the films on (001) $SrTiO_3$ (blue triangles), (001) $LaAlO_3$ (green squares), and (011) $SrTiO_3$ (red circles). Measurements were performed with both the electric currents and magnetic fields along in-plane pseudocubic ⟨100⟩ directions.

[a]Electronic mail: kimdh@ornl.gov

 © 2006 American Institute of Physics
Downloaded 23 Aug 2006 to 128.219.194.241. Redistribution subject to AIP license or copyright, see http://apl.aip.org/apl/copyright.jsp

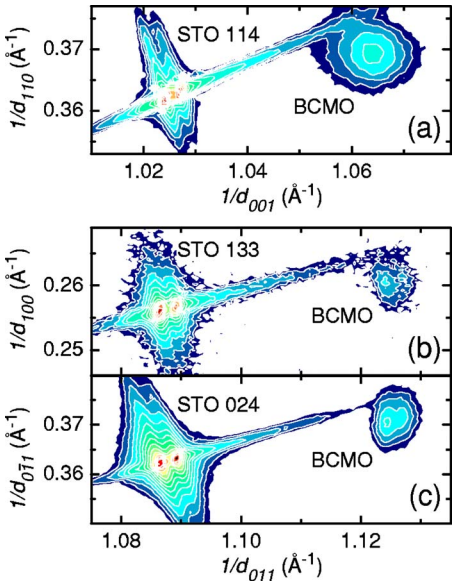

FIG. 2. (Color online) X-ray diffraction reciprocal space maps of $Bi_{0.4}Ca_{0.6}MnO_3$ films on (001) $SrTiO_3$ (a) and (011) $SrTiO_3$ (b and c), containing the $SrTiO_3$ 114 (a), 133 (b), and 024 (c) reflections. The vertical and horizontal axes correspond to the in-plane and out-of-plane directions, respectively. The peak splitting (observed most clearly in the substrate peaks) results from the polychromatic x-ray source (Cu $K\alpha_1$ and Cu $K\alpha_2$ lines).

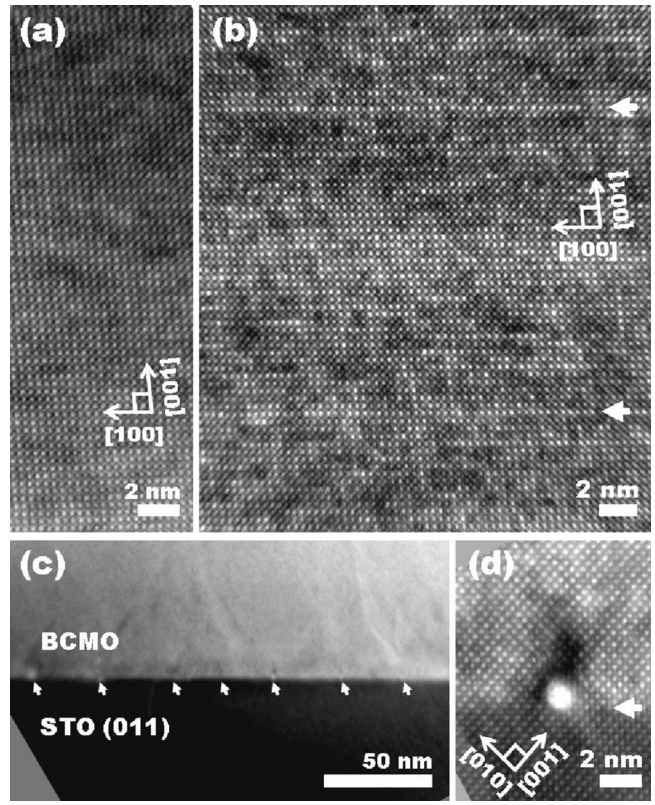

FIG. 3. High resolution Z-contrast STEM cross sections of the $Bi_{0.4}Ca_{0.6}MnO_3$ films: (a) on (001) $LaAlO_3$, and (b) on (001) $SrTiO_3$, where the white arrows indicate single unit-cell-thick, Bi-rich layers. (c) A low resolution image of the film on (011) $SrTiO_3$ substrate, where the arrows indicate regularly spaced misfit dislocations at the film/substrate interface. (d) A high resolution image in the interface region from (c), showing a single misfit dislocation. The white arrow indicates the interface.

Figure 1(a) shows the electrical transport properties of the BCMO films on the different substrates. Turning our attention first to the (001)-oriented substrates, we observe that the film grown on the (001) LAO substrate exhibits a well-defined phase transition near 270 K, significantly lower than the bulk value of 330 K[10] (but consistent with earlier published work.[13] In contrast, the sample grown on (001) STO shows only a very diffuse transition. The corresponding data for the magnetization versus temperature $[M(T)]$ curves for the same samples are shown in Fig. 1(b). Except for a lowering of the transition temperature, the data for BCMO on (001) LAO (green squares) are very similar to that reported for the bulk.[10] The distinct maximum of this curve near 270 K is related to CO, which suppresses local ferromagnetic fluctuations occurring above the CO temperature. In the CO state, antiferromagnetic superexchange interactions between the mixed-valent Mn ions dominate.[10,11] The same magnetization data also allow us to identify the Neel temperature (i.e., the peak near 120 K). In contrast, the film on (001) STO (blue triangles) shows a magnetization that is reduced to half the value observed in the film on (001) LAO and a less-pronounced Neel transition at a slightly lower temperature (100 K). The electrical and magnetic properties of the film on (011) STO [red lines and circles in Figs. 1(a) and 1(b), respectively] are rather similar to those on (001) LAO [but with a more pronounced CO transition at a higher temperature (~285 K)] and are discussed below.

Figure 2(a) shows an XRD reciprocal space map (RSM) around the STO 114 reflection for the BCMO/(001)STO sample. [The sample on (001) LAO exhibits qualitatively similar maps.] Clearly, the film peak is significantly broadened (to the extent that the Cu $K\alpha_1$ and Cu $K\alpha_2$ peaks become indistinguishable, contrary to the substrate diffraction), indicating dispersion in the in-plane and out-of-plane lattice constants.[14] The average pseudocubic lattice constants of the film on (001) LAO are $a=b=3.793$ Å (in plane) and $c=3.833$ Å (out of plane), those for the film on (001) STO substrate are $a=b=3.832$ Å (in plane) and $c=3.762$ Å (out of plane). Note that the crystalline quality is insufficient to determine a deviation with these reciprocal space maps from $\beta=90°$ [corresponding to a doubling of the in-plane lattice parameter along (011) with a splitting of less than 1%].

From these data alone, it is surprising that the film on (001) STO (grown with a slight in-plane tensile strain, but a bulklike $a=b>c$) does not exhibit the transport and magnetization behaviors observed in both the bulk and in the film on (001) LAO (grown under compressive strain, with a near-perfect in-plane lattice match to the substrate, but with $a=b<c$). The opposite behavior would have been expected because the in-plane tensile strain on STO results in a film crystal structure that matches that of the bulk below the CO transition better than that above. However, an investigation of the two samples by Z-STEM [Figs. 3(a) and 3(b)] immediately illustrates fundamental differences. These images, in which the brightness of each atomic column is roughly proportional to Z^2, closely correspond to elemental maps of the Bi content [since $Z(\mathrm{Bi})=83$, $Z(\mathrm{Ca})=20$, and $Z(\mathrm{Mn})=25$].[15] While the Bi distribution within the film on LAO appears to be fairly uniform [Fig. 3(a)], strong segregation is observed in the case of BCMO/(001)STO [Fig. 3(b)]. Highly unusual line-shaped features are observed, corresponding to single unit-cell-thick sheets with enhanced Bi content parallel to the growth surface [white arrows in Fig. 3(b)]. Since these features are not observed in the case of LAO, they may be associated with the tensile nature of the strain. A significantly broadened or even absent CO transition is thus not surpris-

Downloaded 23 Aug 2006 to 128.219.194.241. Redistribution subject to AIP license or copyright, see http://apl.aip.org/apl/copyright.jsp

ing. This type of chemical inhomogeneity on the *A* site has not been reported in any manganite material; further investigation of the resulting properties may yield interesting insights into the correlation between chemical and electronic phase separations.

Growing BCMO on a (011)-oriented substrate results in entirely different strain configurations. Samples on (011) LAO (data not shown) exhibit gradual strain relaxation throughout the film, formation of columnar defects, and correspondingly broadened CO transitions. For BCMO on (011) STO, however, our STEM investigation [Figs. 3(c) and 3(d)] shows a partial strain relief occurring at the film/substrate interface by the formation of regularly spaced misfit dislocations, with the remainder of the film showing few defects and little or no chemical segregation (i.e., a uniform Bi distribution). Figures 2(b) and 2(c) show the corresponding RSM for the STO 133 and 024 reflections to determine the in-plane lattice constants along the [100] and $[0\bar{1}1]$ directions, respectively. Contrary to Fig. 2(a), a measurable splitting of the film peaks into its Cu $K\alpha_1$ and Cu $K\alpha_2$ components indicates a much higher crystalline quality. From these maps, we determine $d_{(011)}=2.668$ Å (out of plane), as well as $d_{(100)}=3.836$ and $d_{(0\bar{1}1)}=2.698$ Å (both in plane), leading to $d_{(001)}=d_{(010)}=[d^2_{(011)}+d^2_{(0\bar{1}1)}]^{1/2}=3.795$ Å. Indexing the film again to obtain $a=b\neq c$, we find $a=c=3.795$ and $b=3.836$ Å, $\gamma=90.6°$. It is interesting to note that the asymmetric tensile strain (along the two in-plane directions, i.e., [100] and $[0\bar{1}1]$) results in a unit cell structure similar to the case of the symmetric compressive strain on (001) LAO. However, the *c* axis is now in the plane of the substrate and the unit cell has a deviation from orthorhombicity. Due to the in-plane asymmetry of the substrate, this $\gamma\neq 90°$ distortion does not require the formation of structural domains. *This additional freedom facilitates the transition to a charge ordered state:* the transport (red lines) and magnetization (red circles) data in Fig. 1 clearly demonstrate a well-defined transition, similar to—but more pronounced than—the case of BCMO/(001)LAO. Temperature-dependent x-ray measurements will need to be performed in order to fully investigate the relationship between the structural transition and the anisotropic strain.

Our observations on BCMO differ significantly from those reported elsewhere for $Nd_{0.5}Sr_{0.5}MnO_3$,[7] a system in which the CO transition is associated with a change of the unit cell such that $a\neq b\neq c$.[16] For BCMO, $a=b$ both above and below the CO transition, which makes it possible to observe CO on the pseudocubically (001)-oriented $LaAlO_3$ substrate. [In $Nd_{0.5}Sr_{0.5}MnO_3$, this transition is only observed on (011) substrates.[7]] However, the data presented here show a clear distinction between films grown onto (001)- and (011)-oriented surfaces, with much better-defined transitions and an anisotropic distortion of the unit cell (i.e., $\gamma\neq 90°$) observed on the (011)-oriented $SrTiO_3$. Furthermore, the comparison between the (001) and (011) STO substrates reveals a striking difference in the way strain is relieved depending on stress symmetry. In particular, the unusual chemical segregation of Bi into single unit-cell-thick sheets is observed exclusively in the BCMO films grown on (001)-oriented $SrTiO_3$, i.e., under tensile stress. Therefore, this work underscores the importance of considering the strain symmetry in addition to simple lattice mismatch.

Research sponsored by the Division of Materials Sciences and Engineering, Office of Basic Energy Sciences, U.S. Department of Energy, under Contract No. DE-AC05-00OR22725 with Oak Ridge National Laboratory, managed and operated by UT-Battelle, LLC.

[1] Y. Konish, Z. Fang, M. Izumi, T. Manako, M. Kasai, H. Kuwahara, M. Kawasaki, K. Terakura, and Y. Tokura, J. Phys. Soc. Jpn. **68**, 3790 (1999).
[2] W. Prellier, A. M. Haghiri-Gosnet, B. Mercey, Ph. Lecoeur, M. Hervieu, Ch. Simon, and B. Raveau, Appl. Phys. Lett. **77**, 1023 (2000).
[3] Y. Tokura and N. Naganosa, Science **288**, 462 (2000).
[4] C. N. R. Rao, A. Arulraj, A. K. Cheetham, and B. Raveau, J. Phys.: Condens. Matter **12**, R83 (2000).
[5] J. G. Belk, J. L. Sudijono, X. M. Zhang, J. H. Neave, T. S. Jones, and B. A. Joyce, Phys. Rev. Lett. **78**, 475 (1997).
[6] Y. Mukunoki, N. Nakagawa, T. Susaki, and H. Y. Hwang, Appl. Phys. Lett. **86**, 171908 (2005).
[7] Y. Wakabayashi, D. Bizen, H. Nakao, Y. Murakami, M. Nakamura, Y. Ogimoto, K. Miyano, and H. Sawa, Phys. Rev. Lett. **96**, 017202 (2005).
[8] Y. Ogimoto, M. Nakamura, N. Takubo, H. Tamaru, M. Izumi, and K. Miyano, Phys. Rev. B **71**, 060403(R) (2005).
[9] Y. Ogimoto, N. Takubo, M. Nakamura, H. Tamaru, M. Izumi, and K. Miyano, Appl. Phys. Lett. **86**, 112513 (2005).
[10] H. Woo, T. A. Tyson, M. Croft, S.-W. Cheong, and J. C. Woicik, Phys. Rev. B **63**, 134412 (2001).
[11] W. Bao, J. D. Axe, C. H. Chen, and S.-W. Cheong, Phys. Rev. Lett. **78**, 543 (1997).
[12] V. A. Bokov, N. A. Grigoryan, and M. F. Bryzhina, Phys. Status Solidi **20**, 745 (1967).
[13] V. N. Smolyaninova, M. Rajeswari, R. Kennedy, M. Overby, S. E. Lofland, L. Z. Chen, and R. L. Greene, Appl. Phys. Lett. **86**, 071922 (2005).
[14] A possible alternative interpretation of this broadening as a consequence of poor epitaxial film-substrate alignment can be ruled out from the narrow rocking curve (normal ω scan). Their full width at half maximums (FWHM) are 0.05° [022 peak of BCMO on (001) LAO], 0.16° [002 peak on (001) STO], and 0.23° [022 peak on (011) STO]. All the substrates show typical rocking curves with their FWHMs smaller than 0.05°.
[15] S. J. Pennycook and L. A. Boatner, Nature (London) **336**, 565 (1988).
[16] H. Kawano, R. Kajimoto, H. Yoshizawa, Y. Tomioka, H. Kuwahara, and Y. Tokura, Phys. Rev. Lett. **78**, 4253 (1997).

Downloaded 23 Aug 2006 to 128.219.194.241. Redistribution subject to AIP license or copyright, see http://apl.aip.org/apl/copyright.jsp